Predictions of nuclear charge radii*

Guang-Sheng Li (李光胜) Cheng Xu (橙许) Man Bao (鲍曼)†

Department of Physics, University of Shanghai for Science and Technology, Shanghai 200093, China

Abstract: In this study, we improve the relations of the charge-radius difference of two isotopes by considering a term that relates to the proton number and the parity of the neutron number. The correction reduces the root-mean-squared deviation to 0.0041 fm for 651 nuclei with a neutron number larger than 20, in comparison with experimental data compiled in the CR2013 database. The improved relations are combined with local relations consisting of the charge radii of four neighboring nuclei. These combinations also prove to be efficient in describing and predicting nuclear charge radii and can reflect the structure evolutions of nuclei. Our predictions of 2467 unknown nuclear charge radii at competitive accuracy, which are calculated using these two types of relations, are tabulated in the Supplemental Material.

Keywords: nuclear charge radii, isotopes, root-mean-squared deviation

DOI: 10.1088/1674-1137/acdb54

I. INTRODUCTION

Nuclear charge radius is one of the fundamental properties of an atomic nucleus and is important in studying the evolution of nuclear structures such as halos and shape transition and coexistence [1−10]. Experimentally, nuclear charge radii can be measured at relatively high precision using various methods, including high energy elastic electron scattering [11, 12], K_α X-ray isotope shifts [13−15], and high-resolution laser spectroscopy [9, 16]. The latest CR2013 experimental database contains 956 root-mean-squared nuclear charge radii of 92 elements from ^{1}H to ^{96}Cm [17, 18].

Theoretically, nuclear charge radii can be calculated using several empirical formulas [19−28], the simplest of which is $1.2A^{1/3}$ fm [29] (where A is the mass number). There are also many microscopic models [30−38], macroscopic-microscopic approaches [39−43], and local or regional methods [44−47] that have been developed to describe and predict nuclear charge radii. For example, the root-mean-squared deviation (RMSD) in describing nuclear charge radii is approximately 0.027 fm for the Skyrme-Hartree-Fock-Bogoliubov (SHFB) model [33], 0.035 fm for the finite-range liquid-drop model (FRLDM) [41], and 0.01 fm for the Garvey-Kelson relations (GK) [44]. In addition, machine learning is also widely used to study nuclear charge radii [48−52].

Recently, two types of methods have been proved to have very high precision in describing and predicting nuclear charge radii. The first is local relations consisting of the charge radii of four neighboring nuclei, denoted by δR_{in-jp} $(i,j=1,2)$ [53, 54]. The descriptive RMSD of δR_{1n-1p} is only 0.0072 fm for 650 nuclei with both neutron and proton numbers larger than 8 [54]. The accuracy can be further improved if four abnormal regions are excluded, as mentioned in Ref. [46]. The second is the relations of the charge-radius difference of two isotopes, denoted by δR_k (where $k\geq 1$ is an integer), and the RMSD for the case of $k=1$ is 0.0050 fm for 651 nuclei with the neutron number larger than 20 and three abnormal regions excluded [55].

This study improves upon the above two types of relations, and this paper is organized as follows: In Sec. II, we improve δR_k by considering a term depending on the proton number and the parity of the neutron number and combine the improved δR_k with the δR_{in-jp} relations. In Sec. III, we investigate the predictive power of our improved relations and predict some unknown nuclear charge radii. Finally, we conclude this paper in Sec. IV.

II. δR_k AND δR_{in-jp} RELATIONS

A. Improved δR_k relations

Let us begin with $\delta R_k(N,Z)$ [55], which is defined as

$$\delta R_k(N,Z) = R(N,Z) - R(N-k,Z) = \sum_{l=0}^{k-1} \delta R_1(N-l,Z)\,, \quad (1)$$

where $R(N,Z)$ is the root-mean-squared charge radius of a

Received 1 March 2023; Accepted 2 June 2023; Published online 3 June 2023

* Supported by National Natural Science Foundation of China (11905130)

† E-mail: mbao@usst.edu.cn

nucleus with neutron number N and proton number Z.

The empirical formula for $\delta R_1(N,Z)$ given by Ref. [55] is

$$\delta R_1^{\rm emp}(N,Z) = a(N-N_0)+b\,,$$
$$a = \begin{cases} a_1,\ N<N_0 \\ a_2,\ N\geq N_0 \end{cases} \tag{2}$$

for $N>20$, where a_1, a_2, and b are optimized parameters, and N_0 equals 24, 39, 66, 109, and 155 for N in the ranges $21\sim28$, $29\sim50$, $51\sim82$, $83\sim126$, and above 127, respectively. For the case of $k>1$, $\delta R_k^{\rm emp}(N,Z)$ is calculated using Eqs. (1)−(2) [55]. Here, nuclei in three abnormal regions should be excluded in the calculation: (1) $N=60$ and $37\leq Z\leq41$; (2) $88\leq N\leq90$ and $62\leq Z\leq67$; (3) $N\leq106$ and $Z=80$, or $N\leq108$ and $Z=78$ or 79 [55].

In Fig. 1 (a), we plot the deviations between the experimental values of δR_1 (denoted by $\delta R_1^{\rm exp}$) and $\delta R_1^{\rm emp}(N,Z)$ calculated using Eq. (2) versus the neutron number N, where the black squares and red circles correspond to even N and odd N, respectively. We can see that the deviations are different for the parity of N.

To reduce the odd-even effect, we consider a Z-dependent correction term and rewrite Eq. (2) as

$$\delta R_1^{\rm emp1}(N,Z) = a(N-N_0)+b+c|Z-Z_0|\,, \tag{3}$$

where c equals c_1 or c_2 for even N or odd N, and Z_0 is the proton number at the half-filled proton shell. The parameters for different neutron shells are given in Table 1, obtained by fitting the experimental values of the nuclear charge radii compiled in the CR2013 database [18]. As shown in Fig. 1 (b), the difference for the parity of N is reduced in the case of $\delta R_1^{\rm exp}-\delta R_1^{\rm emp1}$.

The RMSD (denoted by σ) of δR_k is defined as

$$\sigma = \left\{\frac{1}{\mathbb{N}}[D(N,Z)]^2\right\}^{1/2}, \tag{4}$$

where $D(N,Z)$ is the deviation between the experimental and theoretical values of δR_k, and $\mathbb{N}$ is the total number of $D(N,Z)$ under consideration. According to Eq. (4), σ of Eq. (3) is 0.0041 fm for 651 nuclear charge radii, which is more accurate by approximately 18% compared with that of Eq. (2).

B. Combinations of δR_k and δR_{in-jp}

The δR_{in-jp} $(i,j=1,2)$, proposed based on the independent particle shell model, is defined as [53, 54]

$$\delta R_{in-jp}(N,Z) = R(N,Z)+R(N-i,Z-j) - R(N-i,Z)-R(N,Z-j)\approx 0\,. \tag{5}$$

By substituting Eq. (1) into Eq. (5), we have

Table 1. Optimized parameters a_1, a_2, b, c_1, and c_2 (in units of 10^{-3} fm) in Eq. (3) for different neutron shells, based on the CR2013 database [18].

	a_1	a_2	b	c_1	c_2
$21\leq N\leq28$	−2.475	−2.559	−9.165	4.243	−0.080
$29\leq N\leq50$	−1.740	−0.721	1.586	1.018	0.346
$51\leq N\leq82$	−0.802	−0.346	7.016	0.092	−0.381
$83\leq N\leq126$	−0.459	0.117	2.339	0.175	−0.092
$N\geq127$	−0.044	–	4.822	0.235	0.195

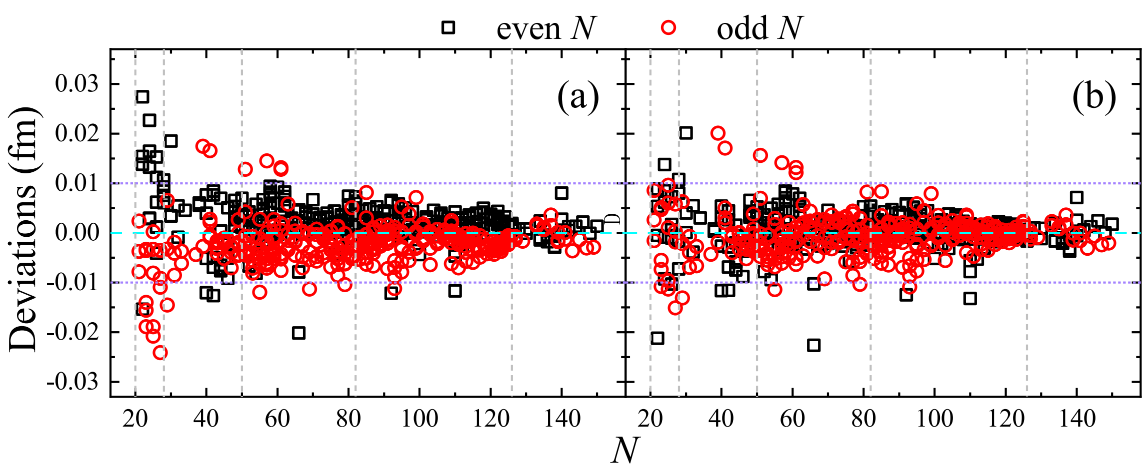

Fig. 1. (color online) Panel (a) is $\delta R_1^{\rm exp}-\delta R_1^{\rm emp}$ versus N, and panel (b) is $\delta R_1^{\rm exp}-\delta R_1^{\rm emp1}$ versus N. The black squares and red circles correspond to even N and odd N, respectively. The gray dashed lines mark the magic numbers of the neutron. The cyan dashed and purple dotted lines are used to guide the eye.

$$\delta R_{in-jp}(N,Z) = R(N,Z) - R(N-i,Z) - \delta R_i(N,Z-j) \approx 0\,. \qquad (6)$$

Here, δR_i can be calculated using Eq. (1), with δR_1 given by Eq. (2) or Eq. (3), and the corresponding calculated δR_{in-jp} is denoted by $\delta R^{\rm emp}_{in-jp}$ or $\delta R^{\rm emp1}_{in-jp}$. Note that the value of $\delta R^{\rm emp}_{in-jp}$ is independent of j because δR_1 given by Eq. (2) is independent of Z.

We label the equation $\delta R_{in-jp} = 0$ with $i = j = 1$, $i = 1$ and $j = 2$, $i = 2$ and $j = 1$, $i = j = 2$ as E_1, E_2, E_3, E_4, respectively. According to Eq. (6), if the value of $R(N,Z)$ or $R(N-i,Z)$ is known, we can calculate the value of the other. Thus, there are up to two possible approaches for each equation to evaluate R of a given nucleus. This leads to the RMSD of the averaged R (denoted by $\overline{\sigma}$), which is defined as

$$\overline{\sigma} = \left[\frac{1}{\mathcal{N}}\sum_{l=1}^{\mathcal{N}}\left(R_l^{\rm exp} - \overline{R}_l^{\rm th}\right)^2\right]^{1/2}, \qquad (7)$$

where $\mathcal{N}$ is the total number of nuclei under consideration, $\overline{R}_l^{\rm th}$ is the averaged value of all available calculated results for the l-th nucleus, and $R_l^{\rm exp}$ is the corresponding experimental value.

Based on the CR2013 database [18], $\overline{\sigma}$ calculated using Eq. (7) for different combinations of $E_1 \sim E_4$ and the corresponding $\mathcal{N}$ are listed in Table 2, for the cases R_{in-jp}, $R^{\rm emp}_{in-jp}$, and $R^{\rm emp1}_{in-jp}$. Here, A_q $(q = 1,2,3,4)$ in rows $2 \sim 5$ and B_q $(q = 1,2)$ in rows $6 \sim 7$ correspond to combinations of two and three equations taken from $E_1 \sim E_4$, respectively, that is, $\overline{R}_l^{\rm th}$ in Eq. (7) is the averaged value of up to four and six possible approaches. The results for the combination of all four equations $E_1 \sim E_4$ are listed in the last row (labeled as "Total"). The last four columns correspond to the results of the same nuclei that can be calculated by A_q or B_q and "Total." The results of B_q and "Total" are invalid for $\delta R^{\rm emp}_{in-jp}$ because of the independence of j, as mentioned above, that is, the value of i should be different for the equations in one combination. As shown in Table 2, the RMSDs of $\delta R^{\rm emp1}_{in-jp}$ and $\delta R^{\rm emp}_{in-jp}$ are smaller than those of δR_{in-jp} by $4\% \sim 39\%$. The optimized combinations are A_1, A_3, and B_1, with the RMSDs of $\delta R^{\rm emp1}_{in-jp}$ as small as that of $\delta R_1^{\rm emp1}$ [see Eq. (3)], while the relatively larger RMSDs of A_2, A_4, B_2, and "Total" may be caused by equation E_4.

Because of the high accuracy of these combinations, the deviations between the experimental and our theoretical values of charge radii should be small. However, there are some exceptions. For example, deviations $R^{\rm exp} - \overline{R}^{\rm th}$ of several isotopes versus N in three different regions are given in Fig. 2 (d), (e), and (f), where $\overline{R}^{\rm th}$ is calculated using combination B_1 of $\delta R^{\rm emp1}_{in-jp}$. The deviations around $N = 60$, 89, and 107 (labeled by gray dashed lines) are relatively larger than the others, which is consistent with the anomalies of the δR_{nn} relation and the linear dependence of R in terms of the valence nucleon numbers, as discussed in Refs. [10, 46]. The anomalies in Fig. 2 (d) and (e) correspond to the sudden increase in R, as shown in Fig. 2 (a) and (b), which is related to the phase transition at $N = 60$, $Z \sim 40$ and the $Z = 64$ subshell [56]; the anomalies in Fig. 2 (f) correspond to the sudden decrease in and obvious odd-even staggering of R, as shown in Fig. 2 (c), which belong to a complex region where deformations, transitions, and shape coexistence exist [57, 58]. This shows that the evolution of nuclear structures can be reflected from these combinations.

III. PREDICTIONS OF NUCLEAR CHARGE RADII

In this section, we investigate the predictive power of

Table 2. RMSDs (in fm) for different combinations of $E_1 \sim E_4$, based on the CR2013 database [18], for the cases R_{in-jp}, $R^{\rm emp}_{in-jp}$, and $R^{\rm emp1}_{in-jp}$. The corresponding number $\mathcal{N}$ of nuclei that can be calculated is also listed. A_q $(q = 1,2,3,4)$ in rows $2 \sim 5$ [B_q $(q = 1,2)$ in rows $6 \sim 7$] correspond to combinations of two (three) equations. A_1: E_1 and E_3; A_2: E_1 and E_4; A_3: E_2 and E_3; A_4: E_2 and E_4; B_1: E_1, E_2 and E_3; B_2: E_1, E_2 and E_4. "Total" in the last row corresponds to the results for the combination of all four equations $E_1 \sim E_4$. The last four columns are the results of the same nuclei that can be calculated by A_q or B_q and "Total."

	$\mathcal{N}$	δR_{in-jp}	$\delta R^{\rm emp}_{in-jp}$	$\delta R^{\rm emp1}_{in-jp}$	$\mathcal{N}$	δR_{in-jp}	$\delta R^{\rm emp}_{in-jp}$	$\delta R^{\rm emp1}_{in-jp}$
A_1	688	0.0055	0.0044	0.0043	548	0.0056	0.0045	0.0045
A_2	773	0.0057	0.0054	0.0053		0.0051	0.0049	0.0049
A_3	739	0.0073	0.0046	0.0045		0.0055	0.0047	0.0046
A_4	649	0.0065	0.0058	0.0057		0.0059	0.0051	0.0051
B_1	750	0.0071	–	0.0043	736	0.0071	–	0.0043
B_2	778	0.0061	–	0.0050		0.0058	–	0.0045
Total	792	0.0060	–	0.0051		0.0056	–	0.0046

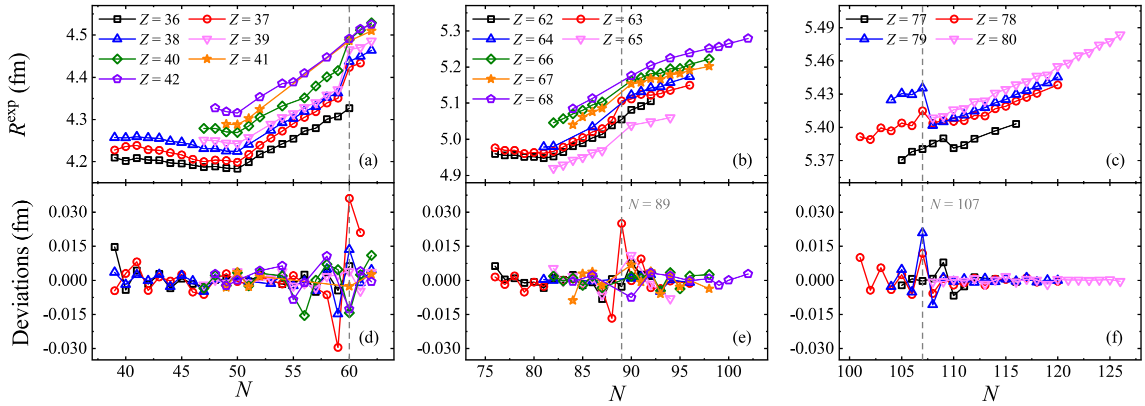

Fig. 2. (color online) Panels (a), (b), and (c) show the charge radii of several isotopes versus N in different regions, and panels (d), (e), and (f) show the corresponding deviations $R^{\rm exp}-\overline{R}^{\rm th}$, where $\overline{R}^{\rm th}$ is calculated using combination B_1 of $\delta R^{\rm emp1}_{in-jp}$. The gray dashed lines are used to guide the eye.

our improved δR_k relations as well as combinations of δR_k and δR_{in-jp}, that is, A_1, A_3, and B_1, as mentioned in Sec. II.B. Here, we consider two extrapolations. The first is from the CR1999 database with 239 experimental nuclear charge radii [59] to the CR2013 database [18], with the RMSD calculated using Eq. (7), denoted by $\sigma_{\rm ex1}$. The second is from the CR2004 database with 692 experimental values [60] to the CR2013 database [18], with the RMSD denoted by $\sigma_{\rm ex2}$. It should be noted that the experimental values in the CR1999 and CR2004 databases are replaced with those in the CR2013 database in both of these extrapolations.

A. Extrapolations of improved δR_k relations

According to Eq. (1), we have

$$R^{\rm pred}_k(N,Z) = R(N-k,Z)+\delta R^{\rm th}_k(N,Z),$$
$$R^{\rm pred}_k(N,Z) = R(N+k,Z)-\delta R^{\rm th}_k(N+k,Z), \qquad (8)$$

where $R^{\rm pred}_k$ is our predicted charge radius, and $\delta R^{\rm th}_k$ can be calculated using Eq. (1) with $k=1\sim15$ and δR_1 given by Eq. (2) or Eq. (3); it can also be calculated using other theoretical databases, as discussed in Ref. [55], the most accurate of which is the WS* model [22]. The theoretical uncertainties of $R^{\rm pred}_k$ are calculated following the method in Ref. [55]. As in Ref. [55], there are up to 30 predictions for a given nucleus on the basis of Eq. (8), and the value with the smallest theoretical uncertainty is taken as our predicted charge radius, that is, $\overline{R}^{\rm th}_l$ in Eq. (7).

Table 3 lists $\sigma_{\rm ex1}$ and $\sigma_{\rm ex2}$ for the same nuclei that can be predicted using Eq. (8) with $\delta R^{\rm th}_k$ calculated based on the WS* model [22], Eq. (2) [55], and Eq. (3). The corresponding number N of nuclei that can be predicted is also listed in parentheses in the first column. Obviously, both $\sigma_{\rm ex1}$ and $\sigma_{\rm ex2}$ for Eq. (3) are smaller than those for Eq. (2). On account of the $N=40$ subshell effect, $\sigma_{\rm ex2}$ of Eq. (2) should decrease to 0.0129 fm with Ga isotopes excluded, as discussed in Ref. [55], while the $N=40$ subshell has no significant effect on $\sigma_{\rm ex2}$ of Eq. (3), which equals 0.0124 fm with Ga isotopes included and is even smaller than that of Eq. (2) with Ga isotopes excluded. Similar to Ref. [55], the average value of the results obtained using Eq. (3) and the WS* model [22] is taken as the theoretical prediction $R^{\rm pre}$ of a given nucleus, and the corresponding theoretical uncertainty $\sigma^{\rm pre}$ is also calculated following the method in Ref. [55].

Table 3. $\sigma_{\rm ex1}$ and $\sigma_{\rm ex2}$ (in fm) of δR_k for the same nuclei that can be calculated using the WS* model [22], Eq. (2) [55], and Eq. (3). The corresponding number N of nuclei that can be predicted are listed in parentheses in the first column.

	WS*	Eq. (2)	Eq.(3)
$\sigma_{\rm ex1}$(464)	0.0133	0.0125	0.0110
$\sigma_{\rm ex2}$(133)	0.0121	0.0148	0.0124

B. Extrapolations of combinations A_1, A_3, and B_1

According to Eq. (6), if the value of $R(N,Z)$ or $R(N-i,Z)$ is known, we can predict the other with $\delta R_i(N,Z-j)$ calculated using Eq. (1) and δR_1 given by Eq. (2) or Eq. (3). For the A_1 or A_3 (B_1) combination, there are up to four (six) predictions of a given nucleus, and the averaged value is taken as our predicted charge radius. $\sigma_{\rm ex1}$ and $\sigma_{\rm ex2}$ of combinations A_1, A_3, and B_1 for the cases δR_{in-jp}, $\delta R^{\rm emp}_{in-jp}$, and $\delta R^{\rm emp1}_{in-jp}$, as well as the corresponding number of nuclei that can be predicted, are given in Table 4. Here, only nuclei that can be predicted by all three relations are considered.

As shown in Table 4, both $\sigma_{\rm ex1}$ and $\sigma_{\rm ex2}$ of δR_{in-jp} are considerably larger than those of the other two types of relations. Although the descriptive RMSDs of $\delta R^{\rm emp}_{in-jp}$ and $\delta R^{\rm emp1}_{in-jp}$ listed in Table 2 are almost the same, $\delta R^{\rm emp1}_{in-jp}$

Table 4. Predictive RMSDs (in fm) of combinations A_1, A_3, and B_1 for the cases δR_{in-jp}, $\delta R^{\rm emp}_{in-jp}$, and $\delta R^{\rm emp1}_{in-jp}$. Columns $2\sim4$ and $5\sim7$ correspond to $\sigma_{\rm ex1}$ and $\sigma_{\rm ex2}$, respectively, for the same nuclei that can be predicted by all three types of relations. The number of nuclei that can be predicted are listed in parentheses on the second row.

	$\sigma_{\rm ex1}$			$\sigma_{\rm ex2}$		
	A_1 (364)	A_3 (327)	B_1 (449)	A_1 (116)	A_3 (122)	B_1 (122)
δR_{in-jp}	0.0146	0.0172	0.0173	0.0144	0.0146	0.0149
$\delta R^{\rm emp}_{in-jp}$	0.0119	0.0146	–	0.0126	0.0125	–
$\delta R^{\rm emp1}_{in-jp}$	0.0110	0.0140	0.0139	0.0107	0.0104	0.0105

gives significantly smaller RMSDs for both of these extrapolations. In the case of $\delta R^{\rm emp1}_{in-jp}$, the values of $\sigma_{\rm ex1}$ and $\sigma_{\rm ex2}$ are almost the same for combinations A_3 and B_1, whereas B_1 can predict considerably more nuclear charge radii. For the same charge radii predicted by A_1, $\sigma_{\rm ex1} = 0.0110$ fm and $\sigma_{\rm ex2} = 0.0105$ fm for B_1, which is as accurate as with our improved δR_k relations (see the last column of Table 3). Thus, combination B_1 is chosen to calculate the theoretical prediction $R^{\rm pre}$ of a given nucleus, and the corresponding theoretical uncertainty $\sigma^{\rm pre}$ is calculated following the method in Ref. [61].

C. Predictions based on the CR2013 database

Considering the high accuracy of the δR_k relations (combination B_1), as discussed in Sec. III.A (Sec. III.B), the charge radii of 2410 (3191) nuclei with $N \geq 20$ and theoretical uncertainties $\sigma^{\rm pre}$ below 0.03 fm, including 1609 (2379) unknowns, are calculated based on the CR2013 database [18] and tabulated in the Supplemental Material [62].

To predict more unknown nuclear charge radii within reasonable theoretical uncertainties, a third method is used to predict nuclear charge radii. This method is the same as combination B_1, except that in each step of extrapolation, the value of R predicted using the δR_k relations should be taken as the prediction of a given nucleus if its theoretical uncertainty $\sigma^{\rm pre}$ is smaller than that of R predicted using combination B_1. Via this method, the charge radii of 3294 nuclei (including 2467 unknowns) are calculated and tabulated in the Supplemental Material [62]. Figure 3 presents the distribution of $\sigma^{\rm pre}$ of nuclear charge radii predicted using the third method, and we find that $\sigma^{\rm pre}$ is smaller than 0.02 fm for most of the nuclei.

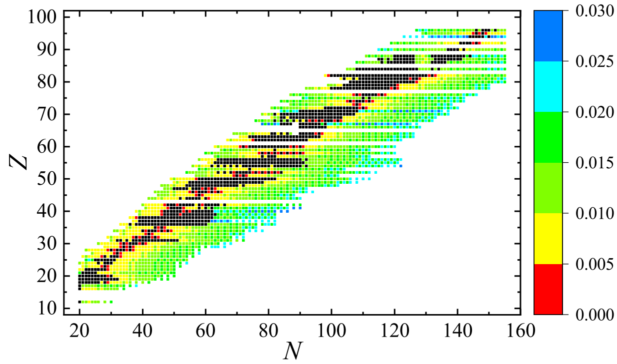

Fig. 3. (color online) Theoretical uncertainties $\sigma^{\rm pre}$ (in fm) of our predicted nuclear charge radii ($\sigma^{\rm pre} < 0.03$ fm), based on the CR2013 database [18]. The black squares denote nuclei with experimental data.

IV. SUMMARY

To summarize, in this paper, we improve the δR_k relations proposed in Ref. [55] by considering a term that relates to Z and the parity of N to reduce the deviations correlating to the odd-even difference of N and combine the improved δR_k with the δR_{in-jp} relations. These two types of relations are proved to be efficient in describing and predicting charge radii for nuclei with $N \geq 20$ and three abnormal regions excluded and are applied to predict 2467 unknown nuclear charge radii with theoretical uncertainties below 0.03 fm, based on the CR2013 database [18]. These predictions are tabulated in the Supplemental Material [62]. In addition, the structure evolutions of nuclei around $N = 60$, 89, and 107 reflected from our improved relations are also discussed.

References

[1] H. De Witte, A. N. Andreyev, N. Barré *et al.*, Phys. Rev. Lett. **98**, 112502 (2007)
[2] Y. A. Lei and J. Y. Zeng, Chin. Phys. C **31**, 731-735 (2007)
[3] W. Nörtershäuser, D. Tiedemann, M. Žáková *et al.*, Phys. Rev. Lett. **102**, 062503 (2009)
[4] I. Angeli, Y. P. Gangrsky, K. P. Marinova *et al.*, J. Phys. G: Nucl. Part. Phys. **36**, 085102 (2009)
[5] T. Yamaguchi, I. Hachiuma, A. Kitagawa *et al.*, Phys. Rev. Lett. **107**, 032502 (2011)
[6] K. T. Flanagan, K. M. Lynch, J. Billowes *et al.*, Phys. Rev. Lett. **111**, 212501 (2013)
[7] M. D. Seliverstov, T. E. Cocolios, W. Dexters *et al.*, Phys. Lett. B **719**, 362-366 (2013)
[8] I. Budinčević, J. Billowes, M. L. Bissell *et al.*, Phys. Rev. C **90**, 014317 (2014)
[9] P. Campbell, I. Moore, and M. Pearson, Prog. Part. Nucl. Phys. **86**, 127-180 (2016)
[10] M. Bao and Q. Wei, Symmetry **13**, 2253 (2021)
[11] H. De Vries, C. De Jager, and C. De Vries, At. Data Nucl. Data Tables **36**, 495-536 (1987)
[12] M. Avgoulea, Y. P. Gangrsky, K. P. Marinova *et al.*, J. Phys. G **38**, 025104 (2011)
[13] F. Boehm and P. L. Lee, At. Data Nucl. Data Tables **14**, 605-611 (1974)
[14] T. Manovitz, R. Shaniv, Y. Shapira *et al.*, Phys. Rev. Lett. **123**, 203001 (2019)

[15] J. Z. Han, C. Pan, K. Y. Zhang *et al*., Phys. Rev. Research **4**, 033049 (2022)
[16] Á. Koszorús, X. F. Yang, W. G. Jiang *et al*., Nat. Phys. **17**, 439 (2021)
[17] I. Angeli and K.P. Marinova, At. Data Nucl. Data Tables **99**, 69-95 (2013)
[18] K. P. Marinova and I. Angeli, http://www-nds.iaea.org/radii/.
[19] J. Duflo, Nucl. Phys. A **576**, 29-64 (1994)
[20] S. Q. Zhang, J. Meng, S. G. Zhou *et al*., Eur. Phys. J. A **13**, 285-289 (2002)
[21] A. E. L. Dieperink and P. Van Isacker, Eur. Phys. J. A **42**, 269 (2009)
[22] N. Wang and T. Li, Phys. Rev. C **88**, 011301(R) (2013)
[23] Y. B. Qian, Z. Z. Ren, and D. D. Ni, Phys. Rev. C **89**, 024318 (2014)
[24] Z. Q. Sheng, G. W. Fan, J. F. Qian *et al*., Eur. Phys. J. A **51**, 40 (2015)
[25] W. H. Ma, J. S. Wang, S. Mukherjee *et al*., Chin. Phys. C **41**, 044103 (2017)
[26] Y. B. Qian and Z. Z. Ren, J. Phys. G: Nucl. Part. Phys. **45**, 085103 (2018)
[27] Y. Y. Cao and J. Y. Guo, Acta Phys. Sin. **69**, 162101 (2020)
[28] T. Li, Y. Luo and N. Wang, At. Data Nucl. Data Tables **140**, 101440 (2021)
[29] A. Bohr and B. R. Mottelson. Nuclear structure: (in 2 volumes) volume i: Single-particle motion, volume ii: Nuclear deformations. (Singapore: World Scientific Publishing Company, 1998)
[30] G. A. Lalazissis, S. Raman, and P. Ring, At. Data Nucl. Data Tables **71**, 1-40 (1999)
[31] M. V. Stoitsov, J. Dobaczewski, W. Nazarewicz *et al*., Phys. Rev. C **68**, 054312 (2003)
[32] S. Goriely, N. Chamel, and J. M. Pearson, Phys. Rev. Lett. **102**, 152503 (2009)
[33] S. Goriely, N. Chamel, and J. M. Pearson, Phys. Rev. C **93**, 034337 (2016)
[34] P. W. Zhao, Z. P. Li, J. M. Yao *et al*., Phys. Rev. C **82**, 054319 (2010)
[35] X. W. Xia, Y. Lim, P. W. Zhao *et al*., At. Data Nucl. Data Tables **121-122**, 1-215 (2018)
[36] K. Y. Zhang, M. K. Cheoun, Y. B. Choi *et al*., At. Data Nucl. Data Tables **144**, 101488 (2022)
[37] R. An, X. Jiang, L. G. Cao *et al*., Phys. Rev. C **105**, 014325 (2022)
[38] R. An, X. Jiang, L. G. Cao *et al*., Chin. Phys. C **46**, 064101 (2022)
[39] F. Buchinger, J. E. Crawford, A. K. Dutta *et al*., Phys. Rev. C **49**, 1402 (1994)
[40] F. Buchinger, J. M. Pearson, and S. Goriely, Phys. Rev. C **64**, 067303 (2001)
[41] F. Buchinger and J. M. Pearson, Phys. Rev. C **72**, 057305 (2005)
[42] H. Iimura and F. Buchinger, Phys. Rev. C **76**, 057302 (2007)
[43] H. Iimura and F. Buchinger, Phys. Rev. C **78**, 067301 (2008)
[44] J. Piekarewicz, M. Centelles, X. Roca-Maza and X. Viñas, Eur. Phys. J. A **46**, 379-386 (2010)
[45] B. H. Sun, C. Y. Liu, and H. X. Wang, Phys. Rev. C **95**, 014307 (2017)
[46] M. Bao, Y. Y. Zong, Y. M. Zhao *et al*., Phys. Rev. C **102**, 014306 (2020)
[47] B. B. Jiao, Acta Phys. Sin. **71**, 152101 (2022)
[48] R. Utama, W. C. Chen, and J. Piekarewicz, J. Phys. G: Nucl. Part. Phys. **43**, 114002 (2016)
[49] Y. F. Ma, C. Su, J. Liu *et al*., Phys. Rev. C **101**, 014304 (2020)
[50] D. Wu, C. L. Bai, H. Sagawa *et al*., Phys. Rev. C **101**, 054323 (2020)
[51] J. Q. Ma and Z. H. Zhang, Chin. Phys. C **46**, 074105 (2022)
[52] X. X. Dong, R. An, J. X. Lu *et al*., Phys. Lett. B **838**, 137726 (2023)
[53] B. H. Sun, Y. Lu, J. P. Peng *et al*., Phys. Rev. C **90**, 054318 (2014)
[54] M. Bao, Y. Lu, Y. M. Zhao *et al*., Phys. Rev. C **94**, 064315 (2016)
[55] C. Ma, Y. Y. Zong, Y. M. Zhao *et al*., Phys. Rev. C **104**, 014303 (2021)
[56] G. J. Fu, M. Bao, Z. He *et al*., Phys. Rev. C **86**, 054303 (2012)
[57] Y. M. Zhao, R. F. Casten, and A. Arima, Phys. Rev. Lett. **85**, 720-723 (2000)
[58] A. E. Barzakh, D. Atanasov, A. N. Andreyev *et al*., Phys. Rev. C **101**, 064321 (2020)
[59] I. Angeli, Table of nuclear root mean square charge radii. INDC(HUN)-033, IAEA Nuclear Data Section, Vienna, 1999
[60] I. Angeli, At. Data Nucl. Data Tables **87**, 185-206 (2004)
[61] G. J. Fu, Y. Lei, H. Jiang *et al*., Phys. Rev. C **84**, 034311 (2011)
[62] Supplemental Material for 2467 predicted charge radii for nuclei with neutron number $N \geq 20$ and theoretical uncertainties below 0.03 fm.